DOI: 10.1002/ejic.200600296

New Polynuclear Mo–Fe Complexes with Ferrocenylamidobenzimidazole Ligands

Paulo N. Martinho,[a,b] Susana Quintal,[a,b] Paulo J. Costa,[a,b] Serena Losi,[c] Vitor Félix,[d] M. Concepción Gimeno,[e] Antonio Laguna,[e] Michael G. B. Drew,[f] Piero Zanello,[c] and Maria José Calhorda*[a,b]

Keywords: Mo^{II} complexes / Ferrocenyl ligands / Polynuclear complexes / DFT calculations / Electrochemistry

The reaction between $[Mo(\eta^3\text{-}C_3H_5)(CO)_2(NCMe)_2Br]$ (**1**) and the ferrocenylamidobenzimidazole ligands $FcCO(NH_2benzim)$ (**L1**) and $(FcCO)_2(NHbenzim)$ (**L2**) led to a binuclear (**2**) and a trinuclear (**3**) Mo–Fe complex, respectively. The single-crystal X-ray structure of $[Mo(\eta^3\text{-}C_3H_5)(CO)_2(L2)Br]$ [L2 = $\{[(\eta^5\text{-}C_5H_5)Fe(\eta^5\text{-}C_5H_4CO)]_2$(2-NH-benzimidazolyl)$\}$] shows that **L2** is coordinated to the *endo* $Mo(\eta^3\text{-}C_3H_5)(CO)_2$ group in a κ^2-N,O-bidentate chelating fashion whereas the Mo^{II} centre displays a pseudooctahedral environment with Br occupying an equatorial position. Complex **2** was formulated as $[Mo(\eta^3\text{-}C_3H_5)(CO)_2(L1)Br]$ on the basis of a combination of spectroscopic data, elemental analysis, conductivity and DFT calculations. **L1** acts as a κ^2-*N*,*N*-bidentate ligand. In both **L1** and **L2**, the HOMOs are mainly localised on iron while the C=O bond(s) contribute to the LUMO(s) and the next highest energy orbitals are Fe–allyl antibonding orbitals. When the ligands bind to $Mo(\eta^3\text{-}C_3H_5)(CO)_2Br$, the greatest difference is that Mo becomes the strongest contributor to the HOMO. Electrochemical studies show that, in complex **2**, no electronic interaction exists between the two ferrocenyl ligands and that the first electron has been removed from the Mo^{II}-centred HOMO.

Introduction

Polynuclear complexes containing molybdenum and iron have received much attention as possible models for the site active metal centre(s) in nitrogenases.[1] In particular, organometallic ligands derived from ferrocene, with one or both the cyclopentadienyl rings properly functionalised with suitable substituents, represent an easy and successful way of designing polynuclear species able to mimic molecules featuring different biological functions or material science properties.[2] Common routes start either from ferrocene carbonyl chloride and an amine, elimination of HCl affording the desired product, or from lithiated ferrocene.[3] Interestingly, both ferrocenium and some ferrocenylalkyl benzimidazoles have been shown to exhibit antitumor properties.[4] A large amount of chemistry has been developed around the ferrocenyl amides, arising from the special biological properties characteristic of amino acids and peptides.[5] Ferrocene labelled amino acids have thus been synthesised,[6] their complexation behaviour towards other metal centres studied[7] and other properties[8] and applications, namely as sensors, investigated.[9] We recently described the synthesis of two new ferrocenylamidobenzimidazole ligands, $FcCO(NH_2benzim)$ (**L1**) and $(FcCO)_2$-(NHbenzim) (**L2**).[10] In this work, we studied their activity as ligands towards the Mo^{II} complex $[Mo(\eta^3\text{-}C_3H_5)(CO)_2(NCMe)_2X]$ (X = halide), **1**,[11] following our interest in the reactivity and properties of Mo^{II} systems.[12,13] Complex **1** has been used as a synthetic precursor for obtaining several types of derivatives, some of which have proved to be suitable catalysts for, among other things, polymerisation of dienes or in organic synthesis for allylic alkylations.[14,15] The complex of **L2** was structurally characterised by single-crystal X-ray diffraction and the other complex by spectroscopic studies. Their redox properties were studied by electrochemical techniques and DFT calculations[16] were carried out to interpret the behaviour upon oxidation and to assign the molecular structure of the complex with **L1**.

[a] Instituto de Tecnologia Química e Biológica (ITQB), Av. da República, EAN,
2781-901 Oeiras, Portugal
[b] Departamento de Química e Bioquímica, Faculdade de Ciências da Universidade de Lisboa,
1749-016 Lisboa, Portugal
E-mail: mjc@fc.ul.pt
[c] Dipartimento di Chimica dell'Università di Siena,
Via Aldo Moro, 53100 Siena, Italy
[d] Departamento de Química, CICECO, Universidade de Aveiro,
3810-193 Aveiro, Portugal
[e] Departamento de Química Inorgánica, Instituto de Ciencia de Materials de Aragón, Universidad de Zaragoza-CSIC,
50009 Zaragoza, Spain
[f] School of Chemistry, University of Reading,
Whiteknights, Reading, RG6 6AD, UK

Results and Discussion

Chemical Studies

The coupling reaction between FcCOCl [Fc = $(\eta^5\text{-}C_5H_5)$-$Fe(\eta^5\text{-}C_5H_4)$] and 2-aminobenzimidazole, $[NH_2(benzimH)]$,

in 1:1 and 2:1 ratios led to the ligands FcCO(NH$_2$benzim) (**L1**) and (FcCO)$_2$(NHbenzim) (**L2**)[10] shown in Scheme 1.

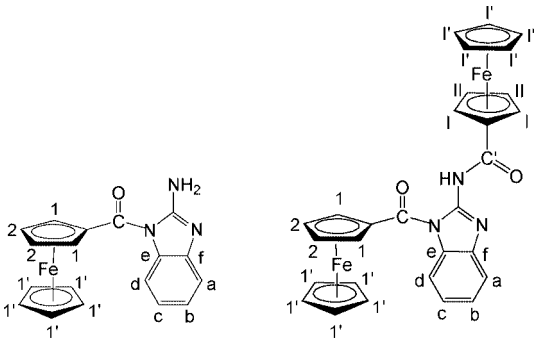

L1 **L2**

Scheme 1.

[Mo(η^3-C$_3$H$_5$)(CO)$_2$(NCMe)$_2$Br], **1**, reacted with the ferrocenyl ligand **L1** in a 1:1 ratio affording, by means of substitution of the acetonitrile ligands, a new complex assigned as [Mo(η^3-C$_3$H$_5$)(CO)$_2$(L1)Br] (**2**) from elemental analysis and spectroscopic data.

The infrared spectrum of **2** shows two very strong bands at 1933 and 1839 cm^{-1}, assigned to the two C≡O stretching modes typical of the carbonyl groups and shifted by 16 and 12 cm^{-1} relative to those in the precursor complex **1**. The $\nu_{C=O}$ stretching frequency can be observed at 1675 cm^{-1} which is essentially the same value as observed in the free ligand (1678 cm^{-1}) suggesting that the carbonyl group does not coordinate to the metal centre. In contrast, both the N–H asymmetric stretches of the NH$_2$ group and the C–NH$_2$ stretch are shifted to lower frequencies, from 3415 cm^{-1} to 3392 cm^{-1} and from 1304 cm^{-1} to 1296 cm^{-1}, respectively. These changes indicate that the NH$_2$ amino group may be coordinated to the molybdenum. The bands assigned to the ferrocenyl subunits appear at 3101 (ν_{C-H}), 1419 (ν_{C-C}), 1107 (asymmetric ring breathing), 1002 $(\delta_{C-H})_{\|}$, 822 $(\pi_{C-H})_{\perp}$, 490 $(\delta_{Fe-Cp})_a$ and 438 cm^{-1} (ν_{Fe-Cp}), i.e. almost in the same positions as in the free ligand which are 3087 (ν_{C-H}), 1450 (ν_{C-C}), 1105 (asymmetric ring breathing), 1000 $(\delta_{C-H})_{\|}$, 823 $(\pi_{C-H})_{\perp}$, 494 $(\delta_{Fe-Cp})_a$ and 440 cm^{-1} (ν_{Fe-Cp}).[17]

The signals in the room temperature ^{1}H NMR spectra of **2** and **3** in [D$_7$]DMF are too broad to be resolved. At room temperature, free rotation across the amide bonds leads to the interconversion between different rotamers of **2** and **3**, with proton resonances occurring on the same time scale. The temperature dependence of the variable hydrogen bonding networks present in the complexes, as seen in the crystal structure of **3** (below), has been reported for several related complexes and explains this behaviour.[6d–f,8] Upon decreasing the temperature to 253 K, the broad signals merge to very well defined signals.

At 253 K, one broad signal at δ = 7.95 ppm can be clearly assigned to the two NH$_2$ protons. This signal is downfield relative to that in the free ligand (δ =6.45 ppm), in agreement with the proposed coordination of the NH$_2$ group to molybdenum.

The Ha, Hb, Hd and Hc protons of the benzimidazole fragment in complex **2** can be seen in the aromatic region at 7.32 (doublet), 7.17 (triplet), 7.08 (doublet) and 6.98 ppm (triplet), respectively. In the free ligand **L1**, they appear at 7.29 (doublet, Ha), 7.06 (Hb), 6.93 (doublet, Hd) and 6.81 ppm (triplet, Hc). The deviations are quite small since these protons are not close to any atom likely to bind to the metal.

The signals of the ferrocenyl unit appear as multiplets (H1, H2 at 5.00, 4.79 ppm) and as a singlet (H1′ at δ = 4.38 ppm), close to the values for the free ligand (two multiplets at 4.89 and 4.53 ppm, and one at δ = 4.22 ppm). The upfield signals at 3.51 (multiplet), 3.30 and 1.18 ppm (doublets) can be assigned, respectively, to the H$_{meso}$, H$_{syn}$ and H$_{anti}$ protons of the allyl fragment. Despite the low global symmetry of the complexes, the signals reflect the local *C*s symmetry of the ferrocenyl ligands. There is no evidence in the NMR spectra for coordinated acetonitrile, suggesting that the two nitrile ligands in the precursor **1** are replaced by **L1**. The methyl signals at δ = 2.19 ppm in the ^{1}H NMR and 1.34 ppm in the ^{13}C NMR spectrum may be assigned to uncoordinated acetonitrile. The low molar conductivity (ΛM = 4.8 Ω^{-1} cm^2 mol^{-1} in dmf) is characteristic of a neutral complex which is expected when two nitriles are lost but not when the bromide and one nitrile are lost. Both the IR and the NMR spectroscopic results thus suggest the coordination of the **L1** ligand in a κ^2-*N*,*N*-bidentate mode in [Mo(η^3-C$_3$H$_5$)(CO)$_2$(L1)Br] (**2**). DFT calculations provided more information on the preferred geometry (see below).

The precursor complex [Mo(η^3-C$_3$H$_5$)(CO)$_2$(NCMe)$_2$Br], **1**, also reacted with the ligand **L2** to give [Mo(η^3-C$_3$H$_5$)(CO)$_2$(L2)Br], **3**, by substitution of the two acetonitrile ligands, as confirmed by single-crystal X-ray diffraction (see below). The infrared spectrum of **3** shows two very strong bands at 1927 and 1830 cm^{-1}, characteristic of the $\nu_{C\equiv O}$ stretching frequencies of the carbonyl groups. Two other very strong bands, at 1704 and 1655 cm^{-1}, can be assigned to C=O stretches. In the free ligand, only one very intense band was observed at 1678 cm^{-1}. The large shift of one band to lower frequency (1655 cm^{-1}) in the complex suggests coordination of one C=O group to molybdenum whereas the other frequency (1704 cm^{-1}) can be assigned to the uncoordinated C=O. The bands assigned to the ferrocenyl subunits appear at 3073 (ν_{C-H}), 1434 (ν_{C-C}), 1107 (asymmetric ring breathing), 1002 $(\delta_{C-H})_{\|}$, 827 $(\pi_{C-H})_{\perp}$ and 495 $(\delta_{Fe-Cp})_a$, approximately in the same positions as in the free ligand.

The ^{1}H NMR spectrum of **3** at 253 K shows one broad signal at δ = 9.10 ppm assigned to one NH proton as well as four signals in the aromatic region at 8.54, 7.75, 7.53 and 7.39 ppm assigned to the Ha, Hb, Hd and Hc protons of the benzimidazole fragment of **L2**. The H1, H2, and H1′ signals of one ferrocenyl unit appear at δ = 4.73, 4.46 and 4.23 ppm with those of the other at δ = 5.13, 4.91 and 4.44 ppm, respectively. The H$_{meso}$, H$_{syn}$ and H$_{anti}$ protons of the allyl fragment can be observed at δ = 3.76, 3.30 and 1.18 ppm, respectively. Unfortunately, the ^{13}C{^{1}H} NMR

spectrum was not of sufficient quality for making assignments.

Crystallography

The X-ray diffraction study of the Mo^{II} complex **3** showed that its crystal structure consists of discrete molecules of $[Mo(\eta^3\text{-}C_3H_5)(CO)_2(L2)Br]$ and disordered CH_2Cl_2 solvent molecules. The chlorine atoms occupy two alternative tetrahedral positions with identical statistical occupancies. Selected bond lengths and angles are given in Table 1.

Table 1. Selected bond lengths [Å] and angles [°] in the molybdenum coordination sphere.

Mo–C(100)	1.934(7)	Mo–C(200)	1.964(8)
Mo–N(11)	2.223(5)	Mo–O(34)	2.225(4)
Mo–Br	2.7169(9)		
C(100)–Mo–C(200)	81.9(3)	C(100)–Mo–N(11)	97.4(2)
C(200)–Mo–N(11)	88.4(2)	C(100)–Mo–O(34)	174.1(2)
C(200)–Mo–O(34)	100.5(2)	N(11)–Mo–O(34)	77.4(2)
C(100)–Mo–Br	93.8(2)	C(200)–Mo–Br	168.1(2)
N(11)–Mo–Br	81.2(1)	O(34)–Mo–Br	82.84(1)

The molecular structure of **3** presented in Figure 1 shows the molybdenum centre to have a pseudo octahedral coordination environment with the centroid of the η^3-allyl ligand and two carbonyl ligands assuming a *fac* arrangement. The **L2** ligand is coordinated in a κ^2-N,O-bidentate chelating fashion with the oxygen atom [O(34)] from a carbonyl group and the N donor atom from the benzimidazole ring occupying equatorial and axial coordination positions, respectively. The Mo–N and Mo–O distances are 2.223(5) and 2.225(4) Å, respectively, leading to a N–Mo–O bite angle of 77.4(2)° for the six-membered chelating ring. The metal coordination sphere is completed by a bromine atom in the equatorial position with a Mo–Br distance of 2.7169(9) Å. This gives rise to the axial isomer depicted in Scheme 2. In addition, in the solid-state, the η^3-allyl ligand adopts an *endo* conformation while the Cp rings of both ferrocenyl subunits display almost eclipsed conformations.

Comparable geometric arrangements with the donor atoms adopting the same spatial disposition around the molybdenum centre have been found for related $Mo^{II}(\eta^3\text{-}C_3H_5)$ complexes.[12,13] To the best of our knowledge, the X-ray structure determination reported here represents the first evidence for the formation of a molybdenum derivative of $(FcCO)_2(NHbenzim)$. The two carbonyl groups from the ligand **L2** adopt a *trans* configuration with the free carbonyl slightly twisted by 79.7(2)° relative to plane of the benzimidazole ring. This arrangement is stabilised by an intramolecular hydrogen bond between the oxygen atom O(20) of the free carbonyl group and the nitrogen atom N(32) from the chelating ring (N–H···O 2.08 Å, 127.0°). The distance between the two iron centres is 7.372(1) Å while the Mo is separated from the iron centres at distances of 5.666(1) and 7.051(1) Å, respectively. These long distances indicate that there is no through-space electronic communication between the three metal centres.

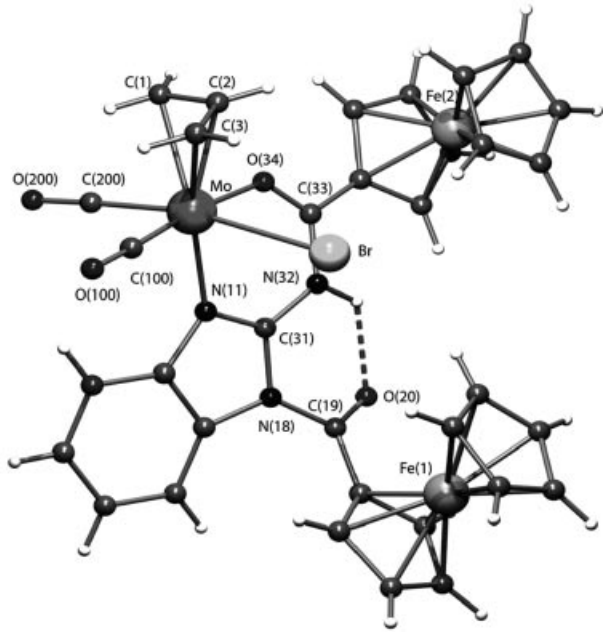

Figure 1. Molecular diagram showing the overall structure of $[Mo(\eta^3\text{-}C_3H_5)(CO)_2(L2)Br]$ (**3**) with the atomic notation scheme used. The labels for the aromatic atoms have been omitted for clarity.

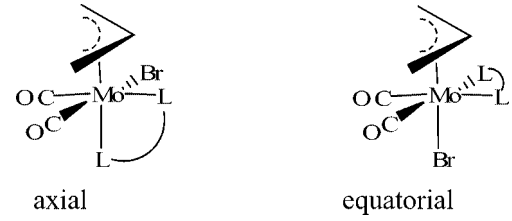

Scheme 2.

DFT Calculations

$[Mo(\eta^3\text{-}C_3H_5)(CO)_2(L1)Br]$ (**2**) can exist as one of two isomers, axial or equatorial (Scheme 2).

DFT[16] calculations (ADF program;[18] see section Computational Details) were performed in order to find the most stable isomer of **2**. The axial isomer (Figure 2) was found to be more stable by 3.2 kcal mol^{-1}. The four-membered ring motif has been found in many related Mo complexes.[19]

The second feature addressed by the DFT calculations was the nature of the frontier orbitals of the ligands **L1** and **L2** and of complexes **2** and **3** in order to further support the electrochemical results described below. The HOMO, LUMO and LUMO+1 of **L1** are shown in Figure 3.

The HOMO and the next levels with lower energy are strongly localised on Fe, as is characteristic of ferrocenes and they represent the orbitals derived from the t_{2g} set of this pseudo octahedral structure of a d^6 species. The LUMO is mainly the π^* orbital of the C=O group while the L+1 orbital is the antibonding Fe–Cp combination involving $x^2–y^2$ and Cp π^*.

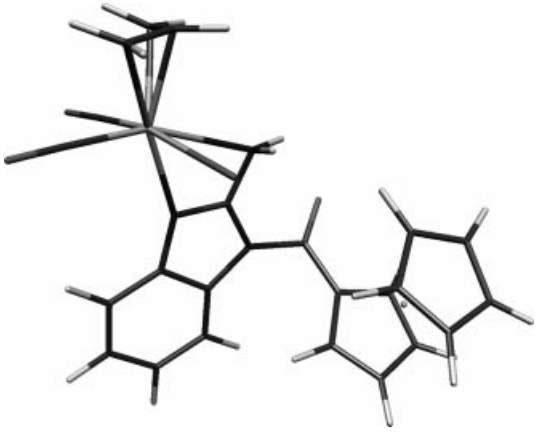

Figure 2. Molekel[20] 3D representation of the structure of the axial isomer of complex **2**, [Mo(η^3-C_3H_5)$(CO)_2$(L1)Br].

$(FcCO)_2$(NHbenzim) (**L2**) has two ferrocenyl groups hanging from the benzimidazole unit. The frontier orbitals are comparable with those of **L1** but their number is double. The HOMO is the analogue of the HOMO of **L1**, localised on one Fc unit, while the H-1 is the same but localised on the second ferrocenyl. The LUMO also has a large contribution of the C=O π* orbital. The Fe–Cp antibonding levels appear at higher energies.

When the ligands bind to the Mo^{II} centre a question about the nature of the HOMO arises, namely, is it localised on Mo or does it remain on Fe? In most known compounds, the higher occupied MOs are Fe orbitals, therefore enabling multiple applications of ferrocenyl derivatives as probes, although there are examples of the opposite behaviour.[21] The most relevant frontier orbitals of complex **2** are depicted in Figure 4.

The HOMO is strongly localised on the $Mo(CO)_2$ fragment, being Mo–C bonding, while the iron based orbitals start at H-1 and continue below. The LUMO is mostly the C=O π* orbital with some Fe contribution.

The same electronic structure can be observed for complex **3** with the HOMO located on $Mo(CO)_2$ and having some contribution from Br. The H-1 is more delocalised with participation of Mo, CO, Br and Fe. H-2 to H-6 are iron d orbitals as in Figure 3 (left). H-7 and H-8, despite a small Fe contribution, are essentially localised on the bromine atom. The LUMO and L+1 are again based on the two C=O π* orbitals, with different proportions of each. Both in the ligands and in their molybdenum complexes, the frontier orbitals are mostly localised on one of the metal atoms.

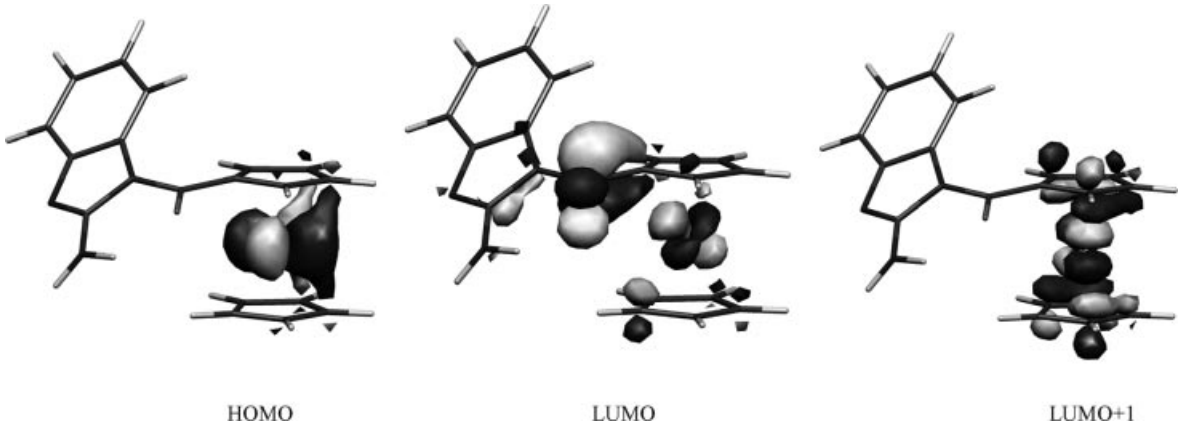

Figure 3. Molekel[20] 3D representation of the HOMO (left), LUMO (centre) and LUMO+1 (right) of FcCO(NH_2benzim) (**L1**).

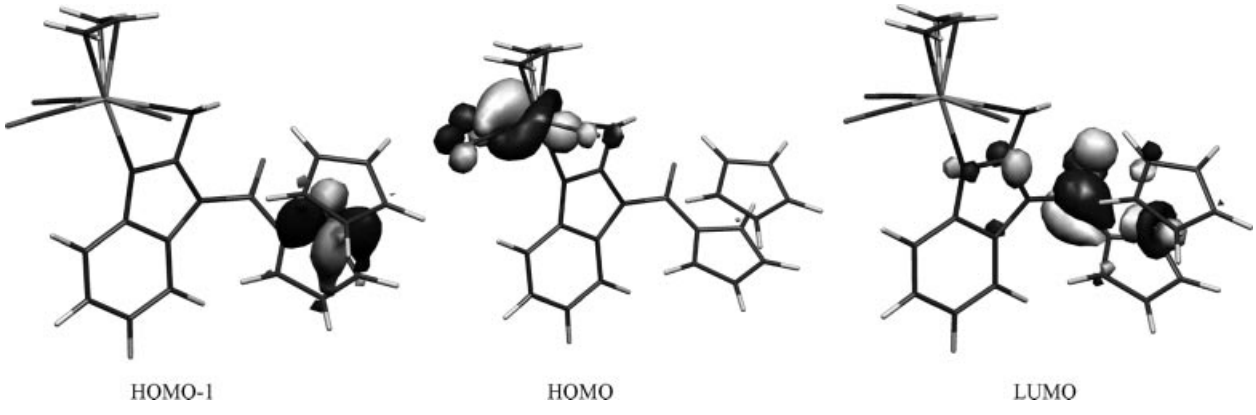

Figure 4. Molekel[20] 3D representation of the HOMO-1 (left), HOMO (centre) and LUMO (right) of [Mo(η^3-C_3H_5)$(CO)_2$(L1)Br], **2**.

Electrochemistry

As deducible from Figure 5, the ferrocene/ferrocenium oxidation exhibited by ligand **L1** is accompanied by chemical complications.

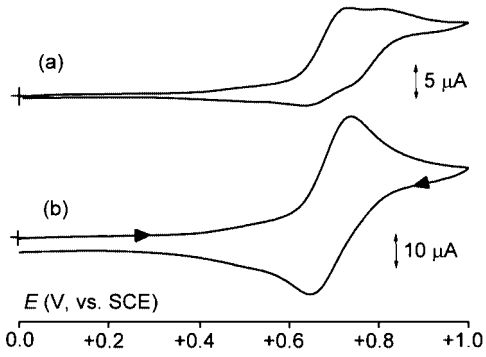

Figure 5. Cyclic voltammetric responses recorded at a platinum electrode in a CH_2Cl_2 solution of **L1** (0.8×10^{-3} mol dm^{-3}). $[NBu_4][PF_6]$ (0.2 mol dm^{-3}) supporting electrolyte. Scan rates: (a) 0.02 V s^{-1}; (b) 0.2 V s^{-1}.

In fact, at very low scan rates two almost overlapping anodic processes appear, which merge in a single process at higher scan rates. In confirmation of the chemical complications following the expected one-electron oxidation, controlled potential coulometric measurements (E_w = +0.9 V) indicated that two electrons *per* molecule are consumed. Even if the closeness of the two processes makes difficult a detailed analysis of the overall process at low scan rates, it is conceivable that the original one-electron oxidation leads to a primary species which converts slowly to a new oxidisable species (ECE mechanism).[22]

It is hence not unexpected that the Mo complex **2**, which further contains the redox-active centres Mo^{II} and Br^-, might afford a more complicated voltammetric pattern, Figure 6. As a matter of fact, three anodic steps can be detected, namely A, B and C. Unfortunately, any attempt to determine the precise number of electrons involved in each step by controlled potential coulometry failed, probably because of both their closeness and the underlying complex electron-transfer mechanisms.

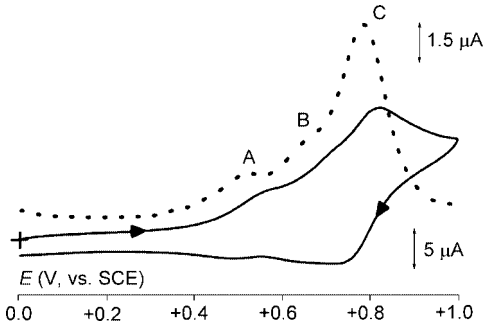

Figure 6. Cyclic (—) and Osteryoung square wave (···) voltammetric responses recorded at a platinum electrode in a CH_2Cl_2 solution of **2** (0.7×10^{-3} mol dm^{-3}). $[NBu_4][PF_6]$ (0.2 mol dm^{-3}) supporting electrolyte. Scan rates: (—) 0.2 V s^{-1}; (···) 0.1 V s^{-1}.

Based on the good extent of chemical reversibility, the most anodic process C can therefore be somewhat naïvely assigned to the ferrocene/ferrocenium oxidation, whereas the process B can be tentatively assigned to the oxidation of the bromide coligand. However, since under the same experimental conditions the free Br^- ion affords two substantially irreversible oxidations[23] (E_p = +0.71 V and +0.94 V, respectively), a contribution to peak C from the second bromide oxidation cannot be ruled out. Finally, in agreement with either the previous findings[24] or the above theoretical calculations, the anodic process A, which also looks likely to exhibit partial chemical reversibility, can be assigned to the Mo^{II}/Mo^{III} couple.

As illustrated in Figure 7, a qualitatively similar situation is exhibited by the diferrocenyl couple **L2/3**.

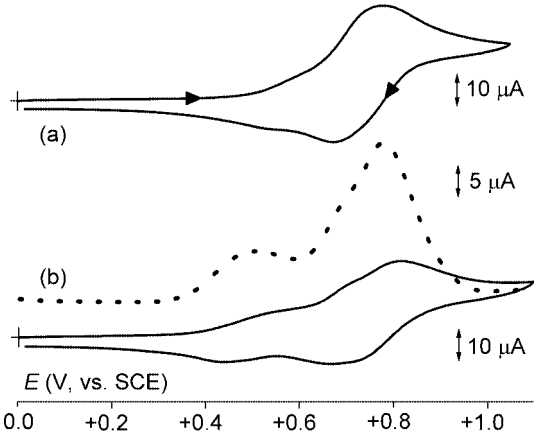

Figure 7. Cyclic (—) and Osteryoung square wave (···) voltammetric responses recorded at a platinum electrode in CH_2Cl_2 solutions of: (a) **L2** (0.7×10^{-3} mol dm^{-3}); (b) **3** (0.6×10^{-3} mol dm^{-3}). $[NBu_4][PF_6]$ (0.2 mol dm^{-3}) supporting electrolyte. Scan rates: (—) 0.2 V s^{-1}; (···) 0.1 V s^{-1}.

Controlled potential coulometric measurements corresponding to the anodic process of **L2** indicate that more than the expected two electrons *per* molecule are consumed (a low level of the electrolytic current still persists even after the consumption of 3.2 electrons per molecule). In this case, however, the final cyclic voltammetric control simply shows partial re-reduction of the oxidised product, which means that the chemical complication could be only due to slow regeneration of the original product likely triggered by traces of water present in the nominally anhydrous solvent. Such a drawback is not unusual in exhaustive electrolysis carried out at relatively high potential values.

It can be noted that the rather rounded peaks exhibited by **L2** give evidence for the postulation that the two ferrocenyl subunits are substantially electronically independent from each other. In turn, as deduced by crystal data, the insertion of the Mo fragment does not modify such electronic interactions.

Table 2 lists the formal electrode potentials for the oxidation of the ferrocenyl fragment in the two series of compounds.

Table 2. Formal electrode potentials (V, vs. the SCE), peak-to-peak separations (mV) and current ratios for the ferrocene/ferrocenium ion oxidation processes in the couples **L1/2** and **L2/3** in CH_2Cl_2 solution.

Complex	$E°'$	ΔE_p [a]	i_{pc}/i_{pa} [a]
L1	+0.69	70	0.86
2	+0.78	70	[b]
L2	+0.72 [c]	93	0.80
3	+0.76 [c]	96	[b]
$Fe(C_5H_5)_2/[Fe(C_5H_5)_2]^+$	+0.39	76	1.0

[a] Measured at 0.1 $V s^{-1}$. [b] Difficult to determine because of close-spaced preceding processes (see text). [c] Nominal two-electron process; from OSWV.

It should be noted that the electron-withdrawing effect exerted by the Mo fragment with respect to the sandwich ligands is, as expected, almost halved on passing from the diferrocenyl to the monoferrocenyl complexes.

Conclusions

The two new ferrocenylamidobenzimidazole ligands $FcCO(NH_2benzim)$ (**L1**) and $(FcCO)_2(NHbenzim)$ (**L2**) react with $[Mo(\eta^3\text{-}C_3H_5)(CO)_2(NCMe)_2Br]$ to afford two polynuclear Mo–Fe complexes. Complex **3**, with the **L2** ligand was structurally characterised by single-crystal X-ray diffraction. The axial isomer was formed and **L2** was coordinated in a κ^2-N,O-bidentate mode using the benzimidazole nitrogen and the closest carbonyl oxygen as donor atoms. The N–H···O hydrogen bond to the second carbonyl of **L2**, already present in the free ligand, was preserved. A combination of spectroscopic data, elemental analysis, conductivity and DFT calculations led us to formulate complex **2** as $[Mo(\eta^3\text{-}C_3H_5)(CO)_2(L1)Br]$ with **L1** coordinating in the neutral form using both the benzimidazole and the NH_2 nitrogen atoms thereby resulting in the most stable axial isomer. The occupied frontier orbitals of the ligands were based on iron, with a LUMO located on the C=O bond(s) and the LUMO+1 being Fe–allyl antibonding. Coordination of the ferrocenyl ligands to Mo leads to Mo based HOMOs, the Fe orbitals coming next and the unoccupied levels being similar to those in the free ligands. In agreement with crystal data and theoretical calculations, electrochemistry shows that in complex **2** no electronic interaction exists between the two ferrocenyl ligands and the first electron is removed from the Mo^{II}-centred HOMO.

Experimental Section

Chemical Studies

Commercially available reagents and all solvents were purchased from standard chemical suppliers. Solvents were dried using common procedures. The syntheses of the molybdenum complexes were carried out under nitrogen using Schlenk tube techniques. The complex $[Mo(\eta^3\text{-}C_3H_5)(CO)_2(NCCH_3)_2Br]$ was synthesised according to literature procedures.[5] The ligands **L1** and **L2** were prepared as described in the literature.[10] Infrared spectra were measured on a Mattson 7000 FT spectrometer. Samples were run as KBr pellets. NMR spectra were recorded on a Bruker Avance-400 spectrometer in $[D_7]$DMF. Electronic spectra were recorded with a UNICAM model UV-4 spectrophotometer. Materials and apparatus for electrochemistry have been described elsewhere.[25] Elemental analyses were carried out at ITQB.

Preparation of $[Mo(\eta^3\text{-}C_3H_5)(CO)_2(L1)Br]$ (2): To a yellow solution of $[Mo(\eta^3\text{-}C_3H_5)(CO)_2(NCCH_3)_2Br]$ (0.177 g, 0.5 mmol) in dichloromethane (10 mL) was added **L1** (0.173 g, 0.5 mmol). The dark-red solution obtained was stirred at room temperature for 3 h. Addition of *n*-hexane resulted in the formation of red solid which was filtered, washed with *n*-hexane and dried under vacuum. Unsuccessful attempts to grow crystals suitable for X-ray diffraction were carried out by vapour diffusion of diethyl ether into a solution of the complex in CH_2Cl_2. Yield 0.274 g (78%). Elemental analysis for $\mathbf{2}\cdot CH_3CN\cdot 0.5CH_2Cl_2$ ($C_{25.5}H_{24}BrClFeMoN_4O_3$) (701.64): calcd. C 43.65, H 3.45, N 7.98; found C 44.12, H 3.51, N 7.73. ^{1}H NMR (400 MHz, $[D_7]$DMF, 253 K): δ = 7.95 (br., NH_2), 7.32 (d, 1 H, Ha), 7.17 (t, 1 H, Hb), 7.08 (d, 1 H, Hd), 6.98 (t, 1 H, Hc), 5.23 (CH_2Cl_2, 1 H), 5.00 (br., 2 H, H1), 4.79 (br., 2 H, H2), 4.38 (br., 5 H, H1′), 3.51 (m, 1 H, H_{meso}), 3.30 (d, 2 H, H_{syn}), 2.19 (s, CH_3CN), 1.18 (d, 2 H, H_{anti}) ppm. ^{13}C NMR (100.6 MHz, $[D_7]$DMF, 253 K): δ = 123.7 (Cb), 120.3 (Cc), 114.7 (Ca), 112.5 (Cd), 75.2 (H_{meso}), 73.1 (C2), 72.3 (C1), 70.9 (C1′), 57.6 ($C_{anti/syn}$), 1.34 (CH_3CN) ppm. UV/Vis (CH_2Cl_2): λ = 482 nm, ε = 1377 $cm^{-1} mol^{-1} dm^3$.

Preparation of $[Mo(\eta^3\text{-}C_3H_5)(CO)_2(L2)Br]$ (3): To a yellow solution of $[Mo(\eta^3\text{-}C_3H_5)(CO)_2(NCCH_3)_2Br]$ (0.177 g, 0.5 mmol) in dichloromethane was added **L2** (0.278 g, 0.5 mmol). The dark-red solution formed was stirred at room temperature for 30 min. Addition of *n*-hexane resulted in the formation of a red solid which was filtered, washed with *n*-hexane and dried under vacuum. Yield 0.382 g (66%). Elemental analysis for $\mathbf{3}\cdot 3CH_2Cl_2\cdot 2CH_3CN$ ($C_{41}H_{40}N_5O_4Cl_6Fe_2BrMo$) (1167.05): calcd. C 42.20, H 3.45, N 6.00; found C 41.73, H 3.26, N 6.00. ^{1}H NMR (400 MHz, $[D_7]$DMF, 253 K): δ = 9.10 (br., NH), 8.54 (d, 1 H, Ha), 7.75 (m, 1 H, Hb), 7.53 (d, 1 H, Hd), 7.39 (t, 1 H, Hc), 5.91 (CH_2Cl_2, 6 H), 5.13 (br., 2 H, HI), 4.91 (br., 2 H, HII), 4.73 (m, 2 H, H1), 4.46 (m, 2 H, H2), 4.44 (s, 5 H, HI′), 4.23 (s, 5 H, H1′), 3.76 (m, 1 H, H_{meso}), 3.30 (d, 2 H, H_{syn}), 2.12 (CH_3CN, 6 H), 1.18 (d, 2 H, H_{anti}) ppm. UV/Vis (CH_2Cl_2): λ = 482 nm, ε = 3750 $cm^{-1} mol^{-1} dm^3$.

Crystallography

Red single-crystals of $[Mo(\eta^3\text{-}C_3H_5)(CO)_2(L2)Br]$ (**3**) of suitable quality for X-ray diffraction were obtained by vapour diffusion of *n*-hexane into a solution of the complex in CH_2Cl_2.

Crystal Data: $C_{35}H_{30}BrCl_2Fe_2MoN_3$, M_r = 915.07; monoclinic, space group $P2_1/n$, Z = 4, a = 15.784(17), b = 12.632(14), c = 18.170(21) Å, β = 105.33(1)°, V = 3494(7), Z = 4, ρ(calc) = 1.740 $Mg m^{-3}$, μ(Mo-K_α) = 2.512 mm^{-1}. X-ray data were collected at room temperature on a MAR research plate system using graphite monochromated Mo-K_α radiation (λ = 0.71073 Å) at Reading University. The crystals were positioned at 70 mm from the image plate. 95 frames were taken at 2° intervals using an appropriate counting time. Data analysis was performed with the XDS program.[26] Intensities were corrected for absorption effects using the DIFABS program.[27] 21894 reflections were collected and merged to 6467 unique reflections giving an R_{int} of 0.0449. The structure was solved by direct methods and by subsequent difference Fourier syntheses and refined by full-matrix least-squares on F^2 using the SHELX-97 system programs.[28] The CH_2Cl_2 solvent molecule was found to be disordered over two positions and the two chlorine atoms were refined in two alternative tetrahedral positions with occupancy factors of 1 – x and x, x being equal to 0.657(9). In addition, the C–Cl distances were constrained at 1.778 Å. Aniso-

tropic thermal parameters were used for the remaining non-hydrogen atoms. The hydrogen atoms bonded to the carbon and nitrogen atoms were included in the refinement in calculated positions with isotropic parameters equivalent to 1.2 times those of the atom to which they are attached. The protons and the hydrogen atoms were not located from the Fourier difference maps and their positions were not included in the refinement. The residual electronic density ranging from –1.157 to 1.480 e Å^{-3} was within expected values. The final refinement of 433 parameters converged to final R and R_w indices $R_1 = 0.0664$ and $wR_2 = 0.1217$ for 5705 reflections with $I > 2\sigma(I)$ and $R_1 = 0.0767$ and $wR_2 = 0.1257$ for all 6467 *hkl* data. Molecular diagrams presented were drawn with the PLATON graphical package software.[29]

CCDC-603243 contains the supplementary crystallographic data for this paper. These data can be obtained free of charge from The Cambridge Crystallographic Data Centre via www.ccdc.cam.ac.uk/data_request/cif.

Computational Details

Density functional calculations[16] were carried out with the Amsterdam Density Functional program (ADF2005).[18] Gradient corrected geometry optimisations,[30] without any symmetry constraints, were performed using the Local Density Approximation of the correlation energy (Vosko, Wilk and Nusair's)[31] and the Generalised Gradient Approximation (Becke Perdew[32,33] exchange and correlation corrections).

A triple-ζ Slater-type orbital (STO) basis set augmented by one polarisation function was used for Mo, Fe, N, O, C and H. A frozen core approximation was used to treat the core electrons: (1s) for N, C and O; ([1–2]s, 2p) for Fe and ([1–3]s, [2–3]p, 3d) for Mo. The calculations were carried out on the crystal structure described above for complex **3** and the structure of L1[10] without any modifications. Geometries for **L2** and complex **2** were based on these structures.

Acknowledgments

We thank FCT for grant POCI/QUIM/58925/2004. PJC acknowledges FCT for grant (SFRH/BD/10535/2002) and SQ for grant (SFRH/BPD/11463/2002). MJC and MCG acknowledge the Acção Integrada Luso-Espanhola (CRUP). PZ gratefully acknowledges the financial support from the University of Siena (PAR 2005). The University of Reading and the EPSRC are thanked for funds for the Image Plate system. MCG and AL thank the Ministerio de Educación y Ciencia (no. CTQ2004-05495-C02-01). We acknowledge the elemental analysis service at the Instituto de Tecnologia Química e Biológica, UNL, Oeiras, Portugal.

[1] J. J. R. Fraústo da Silva, R. J. P. Williams, *The Biological Chemistry of the Elements*, Clarendon Press, Oxford, **1991**.

[2] a) A. Togni, T. Hayashi, *Ferrocenes. Homogeneous Catalysis, Organic Synthesis and Materials Science* (Eds.: A. Togni, T. Hayashi), VCH, Weinheim, **1995**; b) A. Togni, *Metallocenes* (Eds.: A. Togni, R. L. Halterman), Wiley-VCH, Weinheim, **1998**.

[3] a) E. M. Barranco, O. Crespo, M. C. Gimeno, A. Laguna, *Inorg. Chem.* **2000**, *39*, 680; b) S. Canales, O. Crespo, A. Fortea, M. C. Gimeno, P. G. Jones, A. Laguna, *J. Chem. Soc., Dalton Trans.* **2002**, 2250; c) Y. F. Yuan, J. T. Wang, M. C. Gimeno, A. Laguna, P. G. Jones, *Inorg. Chim. Acta* **2001**, *324*, 309; d) E. M. Barranco, O. Crespo, M. C. Gimeno, P. G. Jones, A. Laguna, *J. Chem. Soc., Dalton Trans.* **2001**, 2523.

[4] a) H. Tamura, M. Miwa, *Chem. Lett.* **1997**, 1177; b) D. Osella, M. Ferrali, P. Zanello, F. Laschi, M. Fontani, C. Nervi, G. Cavigiolo, *Inorg. Chim. Acta* **2000**, *306*, 42; c) L. V. Popova, V. N. Babin, Y. A. Beleusov, Y. S. Nekrasov, A. E. Snegireva, N. P. Borodina, G. M. Shaposhnikova, O. B. Bychenko, P. M. Raevskii, M. N. Morozova, A. I. Ilyna, K. G. Shitkov, *Appl. Organomet. Chem.* **1993**, *7*, 85; d) L. V. Snegur, A. A. Simenel, Y. S. Nekrasov, E. A. Morozova, Z. A. Starikova, S. M. Peregudova, Y. V. Kuzmenko, V. N. Babin, L. A. Ostrovskaya, N. V. Bluchterova, M. M. Fomina, *J. Organomet. Chem.* **2004**, *689*, 2473; e) V. N. Babin, P. M. Raevskii, K. G. Snchitkov, L. V. Snegur, Y. S. Nekrasov, *Mendeleev Chem. J.* **1995**, 39.

[5] D. R. van Staveren, N. Metzler-Nolte, *Chem. Rev.* **2004**, *104*, 5931.

[6] a) S. I. Kirin, D. Wissenbach, N. Metzler-Nolte, *New J. Chem.* **2005**, *29*, 1168; b) O. Brosh, T. Weyhermüller, N. Metzler-Nolte, *Inorg. Chem.* **1999**, *38*, 5308; c) X. Hatten, T. Weyhermüller, N. Metzler-Nolte, *J. Organomet. Chem.* **2004**, *689*, 4856; d) A. Hess, O. Brosh, T. Weyhermüller, N. Metzler-Nolte, *J. Organomet. Chem.* **1999**, *589*, 75; e) S. Chowdhury, K. A. Mahmoud, G. Schatte, H.-B. Kraatz, *Org. Biomol. Chem.* **2005**, *3*, 3018; f) F. E. Appoh, T. C. Sutherland, H.-B. Kraatz, *J. Organomet. Chem.* **2004**, *689*, 4669.

[7] a) F. E. Appoh, T. C. Sutherland, H.-B. Kraatz, *J. Organomet. Chem.* **2005**, *690*, 1209; b) O. Brosh, T. Weyhermüller, N. Metzler-Nolte, *Eur. J. Inorg. Chem.* **2000**, 323.

[8] a) K. Heinze, M. Beckmann, *Eur. J. Inorg. Chem.* **2004**, 2974; b) K. Heinze, M. Beckmann, *Eur. J. Inorg. Chem.* **2005**, 3450.

[9] a) H. Shinoara, T. Kusaka, E. Yokota, R. Monden, M. Sisido, *Sens. Actuators B* **2000**, *65*, 144; b) C. Suksai, P. Leeladee, D. Jainuknan, T. Tuntulani, N. Muangsin, O. Chailapakul, P. Kongsaeree, C. Pakavatchai, *Tetrahedron Lett.* **2005**, *46*, 2765; c) A. Berduque, G. Herzog, Y. E. Watson, D. W. M. Arrigan, O. Reynes, G. Royal, E. Saint-Aman, *Electroanalysis* **2005**, *17*, 392; d) H. Miyaji, G. Gasser, S. J. Green, Y. Molard, S. M. Strawbridge, J. H. R. Tucker, *Chem. Commun.* **2005**, 5355.

[10] M. J. Calhorda, P. J. Costa, P. N. Martinho, M. C. Gimeno, A. Laguna, S. Quintal, M. D. Villacampa, *J. Organomet. Chem.* (article accepted).

[11] a) H. Tom Dieck, H. Friedel, *J. Organomet. Chem.* **1968**, *14*, 375; b) R. G. Hayter, *J. Organomet. Chem.* **1967**, *13*, P1; c) P. K. Baker, *Adv. Organomet. Chem.* **1996**, *40*, 45 and references cited therein.

[12] J. R. Ascenso, C. G. de Azevedo, M. J. Calhorda, M. A. A. F. de C. T. Carrondo, P. Costa, A. R. Dias, M. G. B. Drew, V. Félix, A. M. Galvão, C. C. Romão, *J. Organomet. Chem.* **2001**, *632*, 197.

[13] P. M. F. J. Costa, M. Mora, M. J. Calhorda, V. Félix, P. Ferreira, M. G. B. Drew, H. Wadepohl, *J. Organomet. Chem.* **2003**, *687*, 57.

[14] a) F. Dewans, J. Dewailly, J. Meunier- Piret, P. Piret, *J. Organomet. Chem.* **1974**, *76*, 53; b) F. Dewans, E. Goldenberg, *Brevet d'Invention, Inst. Int. Prop. Indust.* **1972**, 2.120.573.

[15] a) B. M. Trost, M. J. Lautens, *Organometallics* **1983**, *2*, 1687; b) B. M. Trost, M. J. Lautens, *J. Am. Chem. Soc.* **1982**, *104*, 5543; c) B. M. Trost, M. J. Lautens, *J. Am. Chem. Soc.* **1982**, *105*, 3343; d) B. M. Trost, M.-H. Hung, *J. Am. Chem. Soc.* **1983**, *105*, 7757.

[16] R. G. Parr, W. Yang, *Density Functional Theory of Atoms and Molecules*, Oxford, University Press, New York, **1989**.

[17] L. Phillips, A. R. Lacey, M. K. Cooper, *J. Chem. Soc., Dalton Trans.* **1988**, 1383.

[18] a) G. te Velde, F. M. Bickelhaupt, S. J. A. van Gisbergen, C. Fonseca Guerra, E. J. Baerends, J. G. Snijders, T. Ziegler, *J. Comput. Chem.* **2001**, *22*, 931; b) C. Fonseca Guerra, J. G. Snijders, G. te Velde, E. J. Baerends, *Theor. Chem. Acc.* **1998**, *99*, 391; c) ADF2005.01, SCM, Theoretical Chemistry, Vrije Universiteit, Amsterdam, The Netherlands.

[19] For instance AMDTMO, AXEGUF, BZATMO, CAPKIN, CAPKOT, DINRAT10, DOLDIR, EBEGIC, FAKBID, GIPTEE, JIDMAK, JOHNAV, NEKFUE, NEKGAL, VAT-

WUU, from the CSD: F. H. Allen, *Acta Crystallogr., Sect. B* **2002**, *58*, 380.
[20] S. Portmann, H. P. Lüthi, *Chimia* **2000**, *54*, 766.
[21] T. Avilés, A. Dinis, J. O. Gonçalves, V. Félix, M. J. Calhorda, Â. Prazeres, M. G. B. Drew, H. Alves, R. T. Henriques, V. da Gama, P. Zanello, M. Fontani, *J. Chem. Soc., Dalton Trans.* **2002**, 4595.
[22] P. Zanello, *Inorganic Electrochemistry. Theory, Practice and Application*, RSC, United Kingdom, **2003**.
[23] G. Dryhurst, P. J. Elving, *Anal. Chem.* **1967**, *39*, 606.
[24] F. Fabrizi de Biani, F. Jäkle, M. Spiegler, M. Wagner, P. Zanello, *Inorg. Chem.* **1997**, *36*, 2103.
[25] E. Stulz, J. K. M. Sanders, M. Montalti, L. Prodi, N. Zaccheroni, F. Fabrizi de Biani, E. Grigiotti, P. Zanello, *Inorg. Chem.* **2002**, *41*, 5269.
[26] W. Kabsch, *J. Appl. Crystallogr.* **1988**, *21*, 916.
[27] DIFABS: N. Walker, D. Stuart, *Acta Crystallogr., Sect. A* **1983**, *39*, 158.
[28] G. M. Sheldrick, *SHELX-97*, University of Göttingen, Germany, **1997**.
[29] A. L. Spek, *PLATON*, *A Multipurpose Crystallographic Tool*, Utrecht University, Utrecht, The Netherlands, **1999**.
[30] a) L. Versluis, T. Ziegler, *J. Chem. Phys.* **1988**, *88*, 322; b) L. Fan, T. J. Ziegler, *Chem. Phys.* **1991**, *95*, 7401.
[31] S. H. Vosko, L. Wilk, M. Nusair, *Can. J. Phys.* **1980**, *58*, 1200.
[32] A. D. Becke, *Phys. Rev. A* **1988**, *38*, 3098
[33] J. P. Perdew, *Phys. Rev. B* **1986**, *33*, 8822.

Received: April 3, 2006
Published Online: August 10, 2006

